AJNR

MR Imaging of Ventral Thalamic Nuclei

K. Yamada, K. Akazawa, S. Yuen, M. Goto, S. Matsushima, A. Takahata, M. Nakagawa, K. Mineura and T. Nishimura

AJNR Am J Neuroradiol published online 19 November 2009
http://www.ajnr.org/content/early/2009/11/19/ajnr.A1870.citation

Published November 19, 2009 as 10.3174/ajnr.A1870

ORIGINAL RESEARCH

MR Imaging of Ventral Thalamic Nuclei

K. Yamada
K. Akazawa
S. Yuen
M. Goto
S. Matsushima
A. Takahata
M. Nakagawa
K. Mineura
T. Nishimura

BACKGROUND AND PURPOSE: The Vim and VPL are important target regions of the thalamus for DBS. Our aim was to clarify the anatomic locations of the ventral thalamic nuclei, including the Vim and VPL, on MR imaging.

MATERIALS AND METHODS: Ten healthy adult volunteers underwent MR imaging by using a 1.5T whole-body scanner. The subjects included 5 men and 5 women, ranging in age from 23 to 38 years, with a mean age of 28 years. The subjects were imaged with STIR sequences (TR/TE/TI = 3200 ms/15 ms/120 ms) and DTI with a single-shot echo-planar imaging technique (TR/TE = 6000 ms/88 ms, b-value = 2000 s/mm^2). Tractography of the CTC and spinothalamic pathway was used to identify the thalamic nuclei. Tractography of the PT was used as a reference, and the results were superimposed on the STIR image, FA map, and color-coded vector map.

RESULTS: The Vim, VPL, and PT were all in close contact at the level through the ventral thalamus. The Vim was bounded laterally by the PT and medially by the IML. The VPL was bounded anteriorly by the Vim, laterally by the internal capsule, and medially by the IML. The posterior boundary of the VPL was defined by a band of low FA that divided the VPL from the pulvinar.

CONCLUSIONS: The ventral thalamic nuclei can be identified on MR imaging by using reference structures such as the PT and the IML.

ABBREVIATIONS: AC = anterior commissure; C = caudate nucleus; CTC = cerebellothalamocortical tract; DBS = deep brain stimulation; DTI = diffusion tensor imaging; FA = fractional anisotropy; fMRI = functional MR imaging; IML = internal medullary lamina; P = putamen; PC = posterior commissure; PT = pyramidal tract; Pulv = pulvinar; RN = red nucleus; ROI = region of interest; ST = sensory tract; STIR = short tau inversion recovery; Th = thalamus; VPL = ventroposterolateral nuclei; Vim = ventrointermediate nuclei

The Vim and VPL are important target regions of the thalamus for DBS. The Vim is the thalamic relay of the CTC; it sends projections primarily to the motor cortex (area 4). This pathway is important for movement control and, thus, has been one of the targets for tremor reduction in patients with Parkinson disease. The VPL relays nociceptive stimuli from the spinothalamic tract to the primary sensory cortex of the parietal lobe (areas 1–3).[1] Damage to this nucleus can cause intractable neuropathic pain,[2] which can be treated with combined DBS of the periaqueductal gray matter and the VPL.[3-5]

Localization of the Vim and the VPL for DBS electrode placement relies mainly on atlas-based stereotactic coordinates, because the direct MR imaging visualization of these nuclei is thought to be difficult. fMRI studies have been able to depict the activation of the VPL, but reproducibility between studies has been limited.[6-9] Furthermore, fMRI is also clinically hampered by long imaging/postprocessing times. Probabilistic tractography obtained through postprocessing of DTI data has been able to successfully segment the thalamus on the basis of its connectivity to various regions of the cerebral cortex.[10-12] However, the substantial variations between subjects, when using the probabilistic approach, seemed to be somewhat problematic when attempting to use this information clinically to guide the electrodes. In this study, we sought to determine whether there is a reliable anatomic landmark that would enable precise localization of the Vim and the VPL by using MR imaging techniques, including the STIR sequence, the color-coded vector map, and FA maps. We also sought to define these structures by combining this information.

Received October 21, 2008; accepted after revision August 12, 2009.

From the Departments of Radiology (K.Y., K.A., S.Y., M.G., S.M., A.T., T.N.), Neurology (M.N.), and Neurosurgery (K.M.), Graduate School of Medical Science, Kyoto Prefectural University of Medicine, Kyoto, Japan.

Please address correspondence to: Kei Yamada, MD, Department of Radiology, Kyoto Prefectural University of Medicine, Kajii-cho, Kawaramachi Hirokoji Agaru, Kamigyo-ku, Kyoto City, Kyoto 602-8566, Japan; e-mail: kyamada@koto.kpu-m.ac.jp

DOI 10.3174/ajnr.A1870

Materials and Methods

Subjects

Ten healthy volunteers, including 5 men and 5 women, ranging in age from 23 to 38 years, with a mean age of 28 years, underwent MR imaging. This study was approved by our institutional review board, and all subjects gave their written informed consent.

Imaging Methods

All images were obtained by using a 1.5T whole-body scanner (Gyroscan Intera; Philips Medical Systems, Best, the Netherlands) with a 6-channel phased-array head coil. The AC and PC were used as the landmarks to determine the axial plane.

The subjects were imaged with a STIR sequences (TR/TE/TI = 3200 ms/15 ms/120 ms; scanning time, 3:09 minutes), with a section thickness of 2.5 mm, matrix size of 256 × 256, and an FOV of 230 mm. DTI scanning was performed with an image-acquisition time of approximately 10 minutes. A single-shot echo-planar imaging technique was used for DTI (TR/TE = 6000 ms/88 ms; scanning time, 3:24 minutes) with a b-value of 2000 s/mm^2. This protocol was run 3 times to perform image averaging to gain a signal intensity–to-noise ratio. Motion-sensitizing gradients were applied in 32 different directions. A parallel imaging technique with an acceleration factor of 3 was used to record the 128 × 37 data points, which were reconstructed to a

BRAIN

ORIGINAL RESEARCH

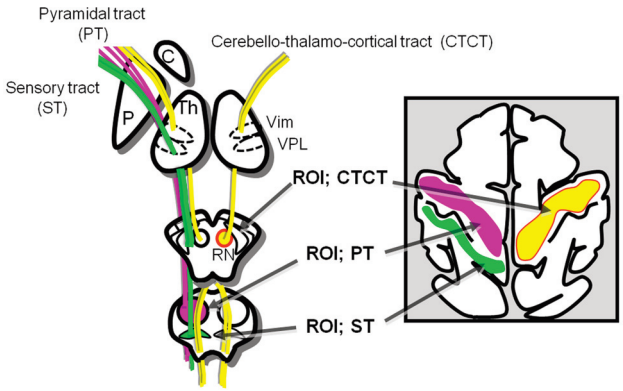

Fig 1. Schematic illustrations of a region-of-interest setting for the ST, PT, and CTC.

128 × 128 resolution. A total of forty-two 2.5-mm-thick sections were obtained without intersection gaps.

Imaging Data Postprocessing

The DTI data were transferred to an off-line workstation for analysis. PRIDE software (Philips Medical Systems, Amsterdam, the Netherlands) was used for motion correction and image analysis. Diffusion tensor elements and anisotropy at each voxel were calculated, and color maps were created.[13,14] Translation of the vectors into neuronal trajectories was achieved by using a previously described method.[15] The procedure for mapping neural connections starts by designating 2 regions of interest in 3D space.

The CTC consists of the dentate projections that cross the midline in the decussation of the superior cerebellar peduncle, which then pass around the red nucleus and enter the Vim of the thalamus. The CTC then projects from the Vim to the primary motor cortex (area 4). To trace the CTC, we placed the region of interest at the ipsilateral red nucleus and white matter adjacent to the primary motor cortex (Fig 1). Tracking of spinothalamic fibers and the PT was performed by placing the regions of interest at the levels of the pons and the primary sensorimotor cortices.

The areas where the CTC and the sensory tracts intersected the thalamus were considered to be the locations of the Vim and the VPL, respectively. These regions of interest were placed by 1 operator for anatomic consistency (K.Y). The stop criteria for the CTC and spinothalamic tracts were FA = 0.1 and angle = 20°-24°. The stop criteria for the PT were FA = 0.4 and angle = 19°.

The tractographic results were superimposed on the STIR images, color-coded vector map, and the FA map to determine whether there was a landmark to identify these structures within the thalamus. Observations were made at the level of the ACPC plane, which represents the ventral part of the thalamus.

Results

Tractography of the CTC and spinothalamic pathway and the PT was successfully performed in all subjects. At the level of the ventral thalamus, the Vim, the VPL, and the PT were all in close contact (Fig 1). The Vim was bounded laterally by the PT. The Vim was in direct contact with the PT in all subjects. The medial landmark was the IML, which was visible on FA and color-coded vector maps as a layer of relatively low anisotropy. The medial border of the Vim did not have direct contact with the IML in almost all subjects (n = 19/20).

The VPL was bounded anteriorly by the Vim, laterally by the internal capsule, and medially by the IML. The posterior boundary of the VPL was defined by a layer of relatively low FA that divided the VPL from the pulvinar. The VPL was in direct contact with the internal capsule and the Vim in all subjects. The medial border of the VPL reached the IML in two-thirds of the subjects (n = 13/20). Both the Vim and the VPL were noted to have slightly diagonal orientations within the thalamus, as illustrated in Figs 2 and 3.

On STIR images, the PT was identified as a small focus of hyperintensity within the posterior limb of the internal capsule. The Vim was noted as a linear area of slight hyperintensity adjacent to the PT (Fig 2). The VPL was noted as an area of slight hypointensity adjacent to the Vim. Both of these structures had diagonally oriented shapes on STIR images, similar to the tractographic results.

Discussion

This study has shown that the Vim and the VPL of the thalamus can be directly identified by combining information from FA and color-coded vector maps. On the atlas of the thalamic nuclei, the locations of the Vim and the VPL are described mainly in correlation with the other surrounding thalamic nuclei. This orthodox way of illustrating the anatomy of the thalamus may not directly help in the in vivo identification of the Vim and the VPL on MR imaging because it is currently not possible to directly localize any of the other thalamic nuclei. The PT, on the other hand, is a well-known conspicuous landmark on MR imaging.[16] If one could use this structure as an internal reference, the locations of the Vim and the VPL would be much easier to identify. The results of the present study show that the Vim is in direct contact with the PT, which is undoubtedly useful additional anatomic information for targeting these nuclei.

The Vim was especially conspicuous on FA maps and was characterized by high anisotropy adjacent to the PT. Although both the Vim and PT have high anisotropy on FA maps, they can be divided into 2 portions on the basis of the location because the PT lies within the posterior limb of the internal capsule and the Vim lies within the thalamus. The high anisotropy of the Vim presumably reflects the highly myelinated nature of this fiber tract, because it plays an important role in controlling movements.

Because the PT can be recognized as a small spot of hyperintensity through the posterior limb of the internal capsule on long TE sequences (eg, STIR), this would become an important landmark when diffusion tensor data are not available. The Vim and the VPL were also depicted on STIR images as stripes of slight hyper- and hypointensities (Fig 2). While it is still unclear why the Vim and the VPL have different signals on STIR, such speculations are beyond the scope of the present study.

The single most important clinical implication of our findings will be in providing anatomic landmarks for precise targeting of DBS electrodes. There are 2 different ways of introducing DBS electrodes: image-based coordinate targeting (direct method) and atlas-based targeting (indirect method).[17-19] Significant differences have been reported between these 2 techniques, with apparently better results by using the direct targeting method.[20]

When using the indirect method, one must register the

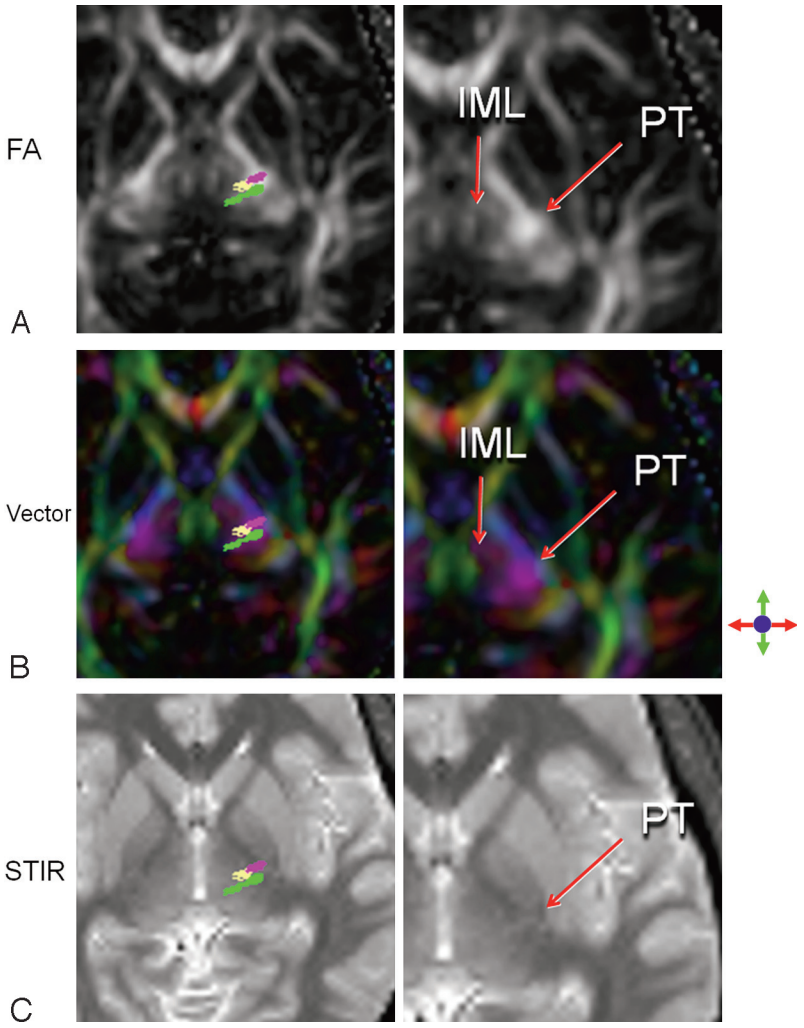

Fig 2. A representative section through the ventral thalamic nuclei is shown. The PT (purple), Vim (yellow), and VPL (green) of the left hemisphere are superimposed on the FA map (*A*), the color-coded vector map (*B*), and the STIR image (*C*). The IML is seen as an area of low FA dividing the medial group of thalamic nuclei from the ventral group. The IML is best appreciated on the color-coded vector map as a dark layer of low anisotropy between the medial nuclei in green (representing the anteroposterior direction) and the ventral groups in purple (representing the superolateral direction). Note that the Vim and VPL can be also identified on the STIR image as an area with diagonally oriented stripes of slight hyper- and hypointensities.

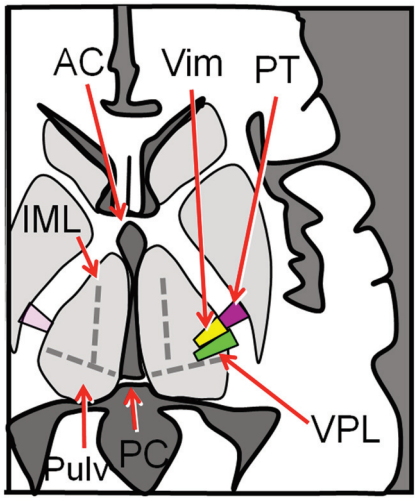

Fig 3. Schematic drawing of the ventral thalamic nuclei and the PT at the level of the ACPC plane. The long axis of the VPL is noted to point toward to the PC, which can be another anatomic landmark to identify this structure within the thalamus.

atlas to the anatomic brain MR images; this is critical because it defines the accuracy. Various warping techniques have been developed, but the "black box" nature of some of these methods limits their practical use in the clinical setting.[21] Another important issue that defines the accuracy of the indirect method is the error due to inaccurate localization of the AC and PC. This error has been estimated to be ≤5 mm, which is unacceptable considering the small size of the targets.[22] Thus, a direct approach would be a more reliable way of performing electrode placement. Our in vivo localization technique now allows direct targeting of the Vim and the VPL, which is preferable for DBS electrode insertion. Direct targeting becomes especially important for gamma knife thalamotomy, a technique also used as a treatment option for movement disorders.[23] Direct image guidance is preferable for gamma knife therapy, because unlike electrode placement, intraoperative electrophysiologic testing of the target location cannot be performed.

The present study has several limitations. First, this is a study of healthy volunteers, so there is no direct clinicoradiologic correlation. Correlation with the results of DBS would be an important step to confirm that the image guidance is truly helpful in accurate electrode placement. Second, only the spinothalamic tracts (the body part of the somatosensory fibers) were depicted by using our tractographic technique, but not the fibers of the trigeminothalamic tract (face/tongue somatosensory fibers). Thus, we were able to depict the VPL but not the ventroposteromedial nucleus, which is known to lie medial to the VPL. This is probably the reason why the VPL did not quite reach the IML in one-third of our subjects. The de-

piction of these face/tongue fibers was not possible owing to the crossing-fiber problem. Tractography is sensitive to large fiber pathways that create more anisotropy. A few previous reports have shown that this problem can be overcome by using advanced techniques.[24-27] Finally, the image distortion of DTI will not be negligible when considering DBS electrode placement. Thus, it would be preferable to use the STIR images instead of DTI data for guidance. Because the contrast of STIR can be adjusted by altering the TI,[28] a future study may be able to define the optimum imaging parameter to better depict these nuclei.

Conclusions

The locations of the Vim and the VPL of the thalamus can be identified by using FA and color-coded vector maps. Our method may provide more accurate targeting for DBS and gamma knife thalamotomy.

Acknowledgments

We are grateful for the technical support provided by Nobuhiro Kakoi, RT, Takamasa Matsuo, RT, Toru Oosawa, RT, Takuji Nishida, RT, Toshiaki Nakagawa, RT, and Yasunori Nakamura, RT. We are also grateful for the valuable comments provided by Naoya Hashimoto, MD, PhD, and Koichi Hosomi, MD, PhD.

References

1. Dostrovsky JO. **Role of thalamus in pain.** *Prog Brain Res* 2000;129:245–57
2. Greenberg E, Treger J, Ring H. **Post-stroke follow-up in a rehabilitation center outpatient clinic.** *Isr Med Assoc J* 2004;6:603–06
3. Hosobuchi Y. **Combined electrical stimulation of the periaqueductal gray matter and sensory thalamus.** *Appl Neurophysiol* 1983;46:112–15
4. Owen SL, Green AL, Stein JF, et al. **Deep brain stimulation for the alleviation of post-stroke neuropathic pain.** *Pain* 2006;120:202–06
5. Nandi D, Aziz T, Carter H, et al. **Thalamic field potentials in chronic central pain treated by periventricular gray stimulation: a series of eight cases.** *Pain* 2003;101:97–107
6. DaSilva AF, Becerra L, Makris N, et al. **Somatotopic activation in the human trigeminal pain pathway.** *J Neurosci* 2002;22:8183–92
7. Davis KD, Kwan CL, Crawley AP, et al. **Functional MRI study of thalamic and cortical activations evoked by cutaneous heat, cold, and tactile stimuli.** *J Neurophysiol* 1998;80:1533–46
8. Becerra LR, Breiter HC, Stojanovic M, et al. **Human brain activation under controlled thermal stimulation and habituation to noxious heat: an fMRI study.** *Magn Reson Med* 1999;41:1044–57
9. Peyron R, Laurent B, García-Larrea L. **Functional imaging of brain responses to pain: a review and meta-analysis.** *Neurophysiol Clin* 2000;30:263–88
10. Ziyan U, Tuch D, Westin CF. **Segmentation of thalamic nuclei from DTI using spectral clustering.** *Med Image Comput Comput Assist Interv Int Conf Med Image Comput Comput Assist Interv* 2006;9(pt 2):807–14
11. Ziyan U, Westin CF. **Joint segmentation of thalamic nuclei from a population of diffusion tensor MR images.** *Med Image Comput Comput Assist Interv Int Conf Med Image Comput Comput Assist Interv* 2008;11:279–86
12. Behrens TE, Johansen-Berg H, Woolrich MW, et al. **Non-invasive mapping of connections between human thalamus and cortex using diffusion imaging.** *Nat Neurosci* 2003;6:750–57
13. Basser PJ, Mattiello J, LeBihan D. **Estimation of the effective self-diffusion tensor from the NMR spin echo.** *J Magn Reson B* 1994;103:247–54
14. Pierpaoli C, Basser PJ. **Toward a quantitative assessment of diffusion anisotropy.** *Magn Reson Med* 1996;36:893–906
15. Mori S, Crain BJ, Chacko VP, et al. **Three-dimensional tracking of axonal projections in the brain by magnetic resonance imaging.** *Ann Neurol* 1999;45:265–69
16. Yagishita A, Nakano I, Oda M, et al. **Location of the corticospinal tract in the internal capsule at MR imaging.** *Radiology* 1994;191:455–60
17. Acar F, Miller JP, Berk MC, et al. **Safety of anterior commissure-posterior commissure-based target calculation of the subthalamic nucleus in functional stereotactic procedures.** *Stereotact Funct Neurosurg* 2007;85:287–91
18. Bootin ML. **Deep brain stimulation: overview and update.** *J Clin Monit Comput* 2006;20:341–46
19. Dormont D, Ricciardi KG, Tandé D, et al. **Is the subthalamic nucleus hypointense on T2-weighted images? A correlation study using MR imaging and stereotactic atlas data.** *AJNR Am J Neuroradiol* 2004;25:1516–23
20. Vayssiere N, Hemm S, Cif L, et al. **Comparison of atlas- and magnetic resonance imaging-based stereotactic targeting of the globus pallidus internus in the performance of deep brain stimulation for treatment of dystonia.** *J Neurosurg* 2002;96:673–79
21. Nowinski WL. **Towards construction of an ideal stereotactic brain atlas.** *Acta Neurochir (Wien)* 2008;150:1–13
22. Nowinski WL. **Anatomical targeting in functional neurosurgery by the simultaneous use of multiple Schaltenbrand-Wahren brain atlas microseries.** *Stereotact Funct Neurosurg* 1998;71:103–16
23. Kondziolka D, Ong JG, Lee JY, et al. **Gamma knife thalamotomy for essential tremor.** *J Neurosurg* 2008;108:111–17
24. Wedeen VJ, Hagmann P, Tseng WY, et al. **Mapping complex tissue architecture with diffusion spectrum magnetic resonance imaging.** *Magn Reson Med* 2005;54:1377–86
25. Frank LR. **Characterization of anisotropy in high angular resolution diffusion-weighted MRI.** *Magn Reson Med* 2002;47:1083–99
26. Tuch DS. **Q-ball imaging.** *Magn Reson Med* 52:1358–72, 2004
27. Yamada K, Sakai K, Hoogenraad FG, et al. **Multitensor tractography enables better depiction of motor pathways: initial clinical experience using diffusion-weighted MR imaging with standard b-value.** *AJNR Am J Neuroradiol* 2007;28:1668–73
28. Nakamura H, Yamada K, Kizu O, et al. **Optimization of TI values in inversion-recovery MR sequences for the depiction of fine structures within gray and white matter: separation of globus pallidus interna and externa.** *Acad Radiol* 2003;10:58–63